

Learning Neural Network Safe Tracking Controllers from Backward Reachable Sets

Yuezhu Xu^a, Mohamed Serry^b, Jun Liu^b, S. Sivaranjani^{a,*}

^a*School of Industrial Engineering, Purdue University, 315 N Grant Street, West Lafayette, 47907, Indiana, USA*

^b*Department of Applied Mathematics, University of Waterloo, 200 University Avenue West, Waterloo, N2L 3G1, Ontario, Canada*

Abstract

The design of tracking controllers that closely follow a reference trajectory while ensuring safety and robustness against disturbances is a challenging problem in the control of autonomous systems. In this work, we propose a neural network-based safe tracking control framework for nonlinear discrete-time systems with reach-avoid specifications in the presence of disturbances. Our approach begins with generation of a nominal trajectory using standard trajectory synthesis approaches, followed by construction of safe zonotopic backward reachable sets along the nominal trajectory. The states lying within the backward reachable sets are guaranteed to satisfy safe reachability specifications. Then, our key insight is to leverage the computed backward reachable sets to inform the architecture and training of a neural network-based tracking controller such that the neural network drives the system's states through these backward reachable sets, thereby improving the likelihood of safe reachability. We perform formal verification with conformal prediction to achieve statistical safety guarantees on the performance of the learned neural controller. The performance of our approach is illustrated through a numerical example on the discrete-time Dubin's car model.

Keywords: Neural Network Control, Safe Control, Reachable Sets

1. Introduction

Control of autonomous systems (e.g., unmanned ground and aerial vehicles) frequently involves reach-avoid tasks, where the system's state needs to be driven safely to a target set, while satisfying specific input and state constraints. Such tasks have to be executed safely, taking into account the presence of model nonlinearity, uncertainties, and disturbances. Reachability control tasks are typically handled by designing nominal trajectories, with associated nominal control inputs, and then embedding tracking controllers into the control system to keep the system's states close to the prescribed nominal trajectories (see, e.g., [1, 2]). Designing tracking controllers that satisfy input and state constraints is a challenging problem, which has been extensively tackled in the literature, e.g., using control barrier functions

[3], control contraction metrics [4–6], and backward reachable sets [7]. In general, existing methods often have computational (e.g., high memory requirement and CPU time) and/or theoretical (e.g., restricted classes of systems and lack of feasibility guarantees) limitations, which motivates further research in this area.

Here, we consider the problem of designing safe tracking controllers for reach-avoid problems in nonlinear discrete-time systems. Specifically, we will employ the notion of backward reachable sets (BRSs) for safe control design. Safe BRSs are sets of states that are guaranteed to be driven to target sets, while satisfying input and state constraints. These sets have been shown to be effective in reach-avoid control tasks [8, 9] and have in fact been used to synthesize safe optimization-based tracking controllers for these tasks under state/input constraints and disturbances [7]. While BRSs provide provable safety and reachability guarantees, the resulting optimization-based tracking controllers may have limited feasibility, as they can only be defined for states that can be driven into the BRSs. Further, such controllers are computationally complex and may have limited applicability especially in real-time applications where fast control evaluation and de-

*Corresponding author. Email: sseetha@purdue.edu

¹The first two authors contributed equally to this manuscript.

²The work of Mohamed Serry and Jun Liu was supported in part by the Natural Sciences and Engineering Research Council of Canada, and in part by the Canada Research Chairs Program.

³The work of Yuezhu Xu and S. Sivaranjani was supported in part by the Air Force Office of Scientific Research grant FA9550-23-1-0492.

ployment are essential.

In this paper, we consider the application of neural networks (NNs) for synthesis of safe tracking controllers for this problem. We are particularly interested in NN-based controllers for two reasons: first, they are well-suited for deployment in online settings, since the computation of control actions involves simple operations once the NN is trained; second, NNs have strong generalization abilities [10], allowing for good performance not only on the training set but on unseen data as well, which is important in maintaining safety under disturbances. These advantages have made NNs a topic of extensive research interest within the control community, with applications to stability verification, stabilization and tracking controller synthesis [11–20].

While training NN-based controllers is a well-studied problem for applications such as stabilization, extending these methods to meet reach-avoid specifications remains challenging due to additional requirements on transient behaviors to reach a target set while avoiding unsafe regions. Therefore, NN controllers trained without explicit guidance on safety and reachability may lead to unsafe or infeasible behaviors. Another key challenge, especially for control tasks, is the availability of ‘good’ data points that can guide the training of NNs to satisfy the required state and input constraints, which are particularly challenging to obtain for complex reach-avoid type specifications.

Motivated by the utility of NNs and BRSs, we propose a new NN-based safe tracking control framework for nonlinear discrete-time systems under disturbances, with training that is guided by BRSs. Our approach can be summarized as follows. We start with a nominal trajectory and associated nominal control input that can be synthesized using standard trajectory generation approaches (e.g., sampling-based and optimization-based methods). We then compute zonotopic safe BRSs along the nominal trajectory that guarantee the satisfaction of safe reachability specifications. We then leverage these sets to guide the training of a NN-based tracking controller, which is designed to push the states through these BRSs, increasing the likelihood of safe tracking during reach-avoid maneuvers. Leveraging already computed BRSs to inform NN training addresses the previously mentioned challenge of generating ‘good’ training data for reach-avoid tasks with state/input constraints. Once trained, our method yields a closed-form NN controller, thus overcoming the computational limitations typically encountered in deploying optimization-based tracking controllers for online tasks. Finally, we employ formal verification with conformal prediction to provide statistical safety guarantees on the tracking per-

formance of the learned neural network controller.

In the literature, reachability analysis has been widely applied to NN control systems, with a primary emphasis on the formal verification of NN-based controller performance. For example, studies such as [21–27] explore reachability analysis for linear systems with neural controllers, or for NN-based models of dynamical systems, focusing largely on computational efficiency and reducing conservativeness. Some recent works have extended these methods to nonlinear systems with neural controllers [28, 29]. However, despite substantial progress in developing reachability-based verification techniques for NN-controlled systems, their practical scalability to high-dimensional systems and long time horizons remains limited, primarily due to the significant nonlinearities introduced by NNs.

In contrast to verification, the use of reachability analysis during the training or synthesis of NN-based controllers is still relatively underexplored. For instance, [30] proposes a set-based training method using zonotopic over-approximations to produce robust neural networks. In [31], a constrained NN training framework based on constrained zonotopes is introduced to ensure that NN outputs avoid predefined unsafe regions. The work in [32] presents a method for learning certifiable NN controllers, paired with a polytopic robust controlled-invariant set, using interval inclusions for systems described by ordinary differential equations. To the best of our knowledge, the current work is among the first to integrate NN-based learning with backward reachability analysis for tracking control in reach-avoid problems, offering a novel direction in the synthesis of safety-aware NN controllers.

The organization of this paper is as follows: the necessary preliminaries and notations are introduced in Section 2, the nonlinear system and the associated tracking problem, with the accompanying assumptions, are presented in Section 3, the proposed method is discussed in Section 4, the performance of the approach is illustrated through a numerical example in Section 5, and future work are discussed in Section 6.

2. Preliminaries and Notations

Let \mathbb{R} , \mathbb{R}_+ , \mathbb{Z} , and \mathbb{Z}_+ denote the sets of real numbers, non-negative real numbers, integers, and non-negative integers, respectively, and $\mathbb{N} = \mathbb{Z}_+ \setminus \{0\}$. Let $[a, b]$, $]a, b[$, $[a, b[$, and $]a, b]$ denote closed, open and half-open intervals, respectively, with end points a and b , and $[a; b]$, $]a; b[$, $[a; b[$, and $]a; b]$ stand for their discrete counterparts, e.g., $[a; b] = [a, b] \cap \mathbb{Z}$, and $[1; 4[= \{1, 2, 3\}$. In

\mathbb{R}^n , the relations $<$, \leq , \geq , and $>$ are defined component-wise, e.g., $a < b$, where $a, b \in \mathbb{R}^n$, iff $a_i < b_i$ for all $i \in [1; n]$. For $a, b \in (\mathbb{R} \cup \{-\infty, \infty\})^n$, with $a \leq b$, the closed hyper-interval (or hyper-rectangle) $\llbracket a, b \rrbracket$ denotes the set $\{x \in \mathbb{R}^n \mid a \leq x \leq b\}$. For $a \in \mathbb{R}$, we define $\lceil a \rceil$ to be the smallest integer no less than a . For $a, b \in \mathbb{R}^n$, $a * b \in \mathbb{R}^n$ represents element-wise multiplication. The n -dimensional vectors with entries of zero and one are denoted by 0_n and 1_n , respectively. For $x \in \mathbb{R}^n$, we define $|x| = [|x_1| \dots |x_n|]^T$. The $n \times n$ identity matrix is denoted id_n . Given $A \in \mathbb{R}^{n \times m}$, $A^\dagger \in \mathbb{R}^{m \times n}$ denotes the Moore-Penrose inverse of A . The space of n -dimensional real vectors is equipped with the maximal norm $\|\cdot\|_\infty$, ℓ_1 -norm $\|\cdot\|_1$, and the Euclidean norm $\|\cdot\|_2$, and \mathbb{B}_n denotes the n -dimensional closed unit ball w.r.t. $\|\cdot\|_\infty$. For $n \times m$ matrices, $\|\cdot\|_\infty$ corresponds to the matrix norm induced by the maximal norm. Given $M, N \subseteq X$, $M \setminus N$ (set difference of M and N) denotes the set $\{x \in M \mid x \notin N\}$, $M + N$ (Minkowski sum of M and N) denotes the set $\{y + z \mid y \in M, z \in N\}$, and $M - N$ (Minkowski or Pontryagin difference of M and N) denotes the set $\{z \in X \mid z + N \subseteq M\}$. The interior of a set $S \subseteq \mathbb{R}^n$ is denoted $\text{int}(S)$. Given $c \in \mathbb{R}^n$ (center), and $G \in \mathbb{R}^{n \times m}$ (generators matrix), the zonotope associated with c and G is the set $c + G\mathbb{B}_m$ (see, e.g., [33]). A standard l -layer feed-forward neural network (NN) structure g is formulated recursively with the number of neurons in layer \mathbf{L}_j being d_j , $j \in [1; l]$ and the input being $z = z^{(0)} \in \mathbb{R}^{d_0}$ as

$$\begin{aligned} \mathbf{L}_j : z^{(j)} &= \phi(v^{(j)}) \quad \forall j \in [1; l-1], \\ \mathbf{L}_l : g(z) &= z^{(l)} = v^{(l)}, \quad z^{(0)} = z, \end{aligned} \quad (1)$$

where $v^{(j)} = W_j z^{(j-1)} + b_j$, and $W_j \in \mathbb{R}^{d_j \times d_{j-1}}$ and $b_j \in \mathbb{R}^{d_j}$ represent the weight and bias for layer \mathbf{L}_j respectively, and $\phi : \mathbb{R}^{d_j} \rightarrow \mathbb{R}^{d_j}$ is a nonlinear activation function that acts element-wise on its argument.

3. Problem Formulation

Consider a discrete nonlinear dynamical system:

$$x_{k+1} \in f(x_k, u_k) + \mathcal{W}, \quad k \in \mathbb{Z}_+, \quad (2)$$

where $x_k \in \mathbb{R}^n$ and $u_k \in \mathbb{R}^m$ are the state and the input at step $k \in \mathbb{Z}_+$, $f : \mathbb{R}^n \times \mathbb{R}^m \rightarrow \mathbb{R}^n$ represents the dynamics of (2), and $\mathcal{W} \subseteq \mathbb{R}^n$ is the disturbance set.

The disturbance set $\mathcal{W} \subseteq \mathbb{R}^n$ is known and given by $\mathcal{W} = \llbracket -\bar{w}, \bar{w} \rrbracket$, $\bar{w} \in \mathbb{R}_+^n$, $u_k \in \mathcal{U}$, $k \in \mathbb{Z}_+$, where $\mathcal{U} = \llbracket \underline{u}, \bar{u} \rrbracket$ is known, and the initial state x_0 belongs to a known set $\mathcal{X}_i = \llbracket \underline{x}_i, \bar{x}_i \rrbracket$. Let $\mathcal{X}_o = \llbracket \underline{x}_o, \bar{x}_o \rrbracket \subseteq \mathbb{R}^n$ be a hyper-rectangular operating domain and $\mathcal{X}_u =$

$\bigcup_{i=1}^{N_u} \llbracket \underline{x}_u^{(i)}, \bar{x}_u^{(i)} \rrbracket \subseteq \mathbb{R}^n$ be an unsafe set defined as a union of N_u hyper-rectangles. We require that the system state is always inside the operating domain, while avoiding the unsafe set. Let $\mathcal{X}_t = \llbracket \underline{x}_t, \bar{x}_t \rrbracket \subseteq \mathbb{R}^n$ be a hyper-rectangular target set that we aim to drive the system's state into from the initial set \mathcal{X}_i .

Assumption 1. *The function f is twice continuously differentiable, and the matrix $D_x f(x, u) \in \mathbb{R}^{n \times n}$ is invertible for all $(x, u) \in \mathcal{X}_o \times \mathcal{U}$, where $D_x f$ denotes the partial derivative of f with respect to x .*

Remark 1. *The Jacobian of f is invertible when f represents the flow map of a continuous-time system. Furthermore, if f is obtained via a numerical time-discretization scheme, such as the forward Euler method, its Jacobian is guaranteed to be invertible provided the time step is chosen sufficiently small. To illustrate this, consider*

$$f(x, u) = x + \Delta_t g(x, u),$$

where $g : \mathbb{R}^n \times \mathbb{R}^m \rightarrow \mathbb{R}^n$ is the vector field of a continuous-time system and is twice continuously differentiable. Then

$$D_x f(x, u) = \text{id}_n + \Delta_t D_x g(x, u). \quad (3)$$

With the condition

$$\Delta_t < \frac{1}{\sup_{(x,u) \in \mathcal{X}_o \times \mathcal{U}} \|D_x g(x, u)\|_\infty}, \quad (4)$$

we have that the matrix $D_x f(x, u)$ is invertible for all $(x, u) \in \mathcal{X}_o \times \mathcal{U}$. In this case, invertibility follows from the Neumann-series criterion $\|\Delta_t D_x g(x, u)\|_\infty < 1$, which ensures that $\text{id}_n + \Delta_t D_x g(x, u)$ is nonsingular uniformly over the domain.

Assumption 2. $\mathcal{X}_i \subseteq \mathcal{X}_o \setminus \mathcal{X}_u$ and $\mathcal{X}_t \subseteq \mathcal{X}_o \setminus \mathcal{X}_u$.

Let $N \in \mathbb{N}$ and $[0; N]$ be a finite-time horizon over which the reach-avoid specifications above are to be satisfied for system (2), assuming zero disturbance. Specifically, let $\{\tilde{x}_k\}_{k=0}^N$ and $\{\tilde{u}_k\}_{k=0}^{N-1}$ be given nominal state and input sequences. Note that such nominal state and input sequences can be constructed by means of standard trajectory generation approaches such as RRT [34] or trajectory optimization [35–38]. The nominal state and input sequences are designed to satisfy:

$$\begin{aligned} \tilde{x}_{k+1} &= f(\tilde{x}_k, \tilde{u}_k), \quad k \in [0; N-1] \\ \tilde{u}_k &\in \mathcal{U}, \quad k \in [0; N-1], \\ \tilde{x}_k &\in \text{int}(\mathcal{X}_o) \setminus \mathcal{X}_u, \quad k \in [0; N], \\ \tilde{x}_0 &\in \mathcal{X}_i, \quad \tilde{x}_N \in \text{int}(\mathcal{X}_t). \end{aligned}$$

We state the safe tracking control design problem here.

Problem 1. Given the nominal sequences $\{\tilde{x}_k\}_{k=0}^N$ and $\{\tilde{u}_k\}_{k=0}^{N-1}$, find a NN control law $\mu : \mathbb{R}^n \times [0; N-1] \rightarrow \mathcal{U}$ that drives the states of system (2) from the initial set \mathcal{X}_i to the target set \mathcal{X}_t in N steps, while staying in the operating domain \mathcal{X}_o and avoiding the unsafe set \mathcal{X}_u .

4. Neural-Network Tracking Control using Backward Reachable Sets

We now present our NN-based tracking control framework, which consists of first constructing backward reachable sets (BRSS) and then using them to guide the training of NN controllers.

4.1. Backward Reachable Sets

In this section, we briefly outline the computations of BRSSs, following the approach in [7]. We first construct an initial state tube that consists of the hyper-rectangles:

$$\mathcal{T}_{x,k} = \tilde{x}_k + \llbracket -R_{x,k}, R_{x,k} \rrbracket, R_{x,k} \in \mathbb{R}_+^n, k \in [0; N],$$

satisfying:

$$\begin{aligned} \mathcal{T}_{x,k} &\subseteq \mathcal{X}_o \setminus \mathcal{X}_u, k \in [0; N-1], \\ \mathcal{T}_{x,N} &\subseteq \mathcal{X}_t. \end{aligned}$$

We also construct an initial input tube consisting of the hyper-rectangles:

$$\mathcal{T}_{u,k} = \tilde{u}_k + \llbracket -R_{u,k}, R_{u,k} \rrbracket \subseteq \mathcal{U}, R_{u,k} \in \mathbb{R}_+^m, k \in [0; N-1].$$

These tubes ensure satisfaction of the state and input constraints and are also used to quantify linearization errors. Next, the nonlinear dynamics (2) is conservatively linearized along the nominal states and inputs as follows. We define, for $k \in [0; N-1]$,

$$\begin{aligned} A_k &:= D_x f(\tilde{x}_k, \tilde{u}_k), \\ B_k &:= D_u f(\tilde{x}_k, \tilde{u}_k), \\ c_k &:= f(\tilde{x}_k, \tilde{u}_k) - A_k \tilde{x}_k - B_k \tilde{u}_k, \end{aligned}$$

where $D_u f$ denotes the partial derivative of f with respect to u . Note that A_k is invertible for all $k \in [0; N-1]$ due to the invertibility assumption on $D_x f$ in Section 3.

For a fixed $k \in [0; N-1]$ and state and input hyper-rectangles $T_{x,k} = \tilde{x}_k + \llbracket -r_x, r_x \rrbracket, r_x \in \mathbb{R}_+^n$, and $T_{u,k} = \tilde{u}_k + \llbracket -r_u, r_u \rrbracket, r_u \in \mathbb{R}_+^m$, we define the set $\mathcal{W}(T_{x,k}, T_{u,k}) \subseteq \mathbb{R}^n$ such that it over-estimates the linearization errors over $T_{x,k}$ and $T_{u,k}$ and accounts for the disturbance set \mathcal{W} . Particularly,

$$\mathcal{W}(T_{x,k}, T_{u,k}) := \mathcal{W} + \llbracket -\mathbf{e}(T_{x,k}, T_{u,k}), \mathbf{e}(T_{x,k}, T_{u,k}) \rrbracket,$$

where

$$(\mathbf{e}(T_{x,k}, T_{u,k}))_i := \frac{1}{2} [r_x^\top, r_u^\top] \bar{\mathbf{H}}_{f_i}(T_{x,k}, T_{u,k}) [r_x; r_u],$$

$i \in [1; n]$. Herein, $\bar{\mathbf{H}}_{f_i}(T_{x,k}, T_{u,k}) \in \mathbb{R}^{(n+m) \times (n+m)}$ is a matrix that satisfies:

$$(\bar{\mathbf{H}}_{f_i}(T_{x,k}, T_{u,k}))_{p,q} \geq \sup_{T_{x,k} \times T_{u,k}} |(\text{Hess}[\mathcal{F}_i](\cdot))_{p,q}|,$$

$p, q \in [1; n+m]$, where $\mathcal{F} : \mathbb{R}^{n+m} \rightarrow \mathbb{R}^n$ is defined as $\mathcal{F}([x^\top, u^\top]^\top) = f(x, u)$, $(x, u) \in \mathbb{R}^n \times \mathbb{R}^m$, and $\text{Hess}[\mathcal{F}_i](z)$ denotes the Hessian of \mathcal{F}_i evaluated at z (recall the twice-differentiability assumption on f).

Incorporating \mathbf{W} ensures over-approximation of the nonlinear dynamics (2) using the linearized dynamics as highlighted in the following lemma.

Lemma 1. For all $(x, u) \in T_{x,k} \times T_{u,k}$,

$$f(x, u) + \mathcal{W} \subseteq A_k x + B_k u + c_k + \mathbf{W}(T_{x,k}, T_{u,k}).$$

With the linearized dynamics, we compute under-approximate zonotopic BRSSs and simultaneously optimize the state and input tubes in order to maximize the sizes of the resulting BRSSs. This yields zonotopic safe BRSSs, Λ_k , $k \in [0; N]$, of the form:

$$\Lambda_k = \tilde{x}_k + G^k \mathbb{B}_{q_k}, G^k \in \mathbb{R}^{n \times q_k}, q_k \in \mathbb{N}, k \in [0; N],$$

an *optimized* input tube consisting of hyper-rectangles

$$T_{u,k} = \tilde{u}_k + \llbracket -r_{u,k}, r_{u,k} \rrbracket \subseteq \mathcal{T}_{u,k} \subseteq \mathcal{U}, r_{u,k} \in \mathbb{R}_+^m,$$

$k \in [0; N-1]$, and an *optimized* state tube consisting of hyper-rectangles

$$T_{x,k} = \tilde{x}_k + \llbracket -r_{x,k}, r_{x,k} \rrbracket \subseteq \mathcal{T}_{x,k}, r_{x,k} \in \mathbb{R}_+^n,$$

$k \in [0; N-1]$. The BRSSs Λ_i , $i \in [0; N]$ are defined such that:

$$\begin{aligned} \Lambda_N &= T_{x,N}, \\ \Lambda_k &\subseteq A_k^{-1}(\Psi_k + (-(c_k + B_k T_{u,k}))) \cap T_{x,k}, \end{aligned}$$

$k \in [0; N-1]$, where Ψ_k satisfies:

$$\Psi_k \subseteq (\Lambda_{k+1} - \mathcal{W}(T_{x,k}, T_{u,k})).$$

Each set Λ_k under-approximates the safe BRS (located in the safe hyper-rectangle $T_{x,k}$), starting from Λ_{k+1} under the conservatively linearized dynamics with input values in $T_{u,k}$.

To account for the effect of the disturbances represented by set \mathcal{W} , the BRSs are accompanied by their deflated versions:

$$\tilde{\Lambda}_k = \tilde{x}_k + \tilde{G}^k \mathbb{B}_{q_k} \subseteq \Lambda_k - \mathcal{W}, \quad \tilde{G}^k \in \mathbb{R}^{n \times q_k}, \quad k \in [0; N],$$

The sets $\tilde{\Lambda}_k$ and Ψ_k are acquired by under-approximating Minkowski differences, with employment of the method in [7, Lemma 7]. The construction of the sequence of BRSs $\{\Lambda_k\}_{k=0}^N$, the deflated version $\{\tilde{\Lambda}_k\}_{k=0}^N$, the state and input sequences $\{\mathbb{T}_{x,k}\}_{k=0}^N$ and $\{\mathbb{T}_{u,k}\}_{k=0}^{N-1}$ provides the following safety and reachability guarantees.

Theorem 1. *For all $k \in [0; N - 1]$, $\Lambda_k \subseteq \mathcal{X}_o \setminus \mathcal{X}_u$, $x \in \Lambda_k \Rightarrow \exists u \in \mathbb{T}_{u,k} \subseteq \mathcal{U}$ s.t. $f(x, u) \in \tilde{\Lambda}_{k+1} \Rightarrow f(x, u) + \mathcal{W} \subseteq \Lambda_{k+1}$, and $\Lambda_N \subseteq \mathcal{X}_t$.*

The proofs of Lemma 1 and Theorem 1 follow along the lines of [7] and are omitted for brevity.

4.2. Architecture Design and Training of Neural Tracking Controllers

With the BRSs, namely Λ_k , $k \in [0; N]$ computed⁴, we aim to obtain a NN tracking controller $\mu : \mathbb{R}^n \times [0; N - 1] \rightarrow \mathcal{U}$ that drives the states in Λ_k towards the center of $\tilde{\Lambda}_{k+1}$, that is, \tilde{x}_{k+1} , $k \in [0; N - 1]$. For each step k , $\mu(\cdot, k)$ is designed to have a NN architecture with feed-forward and multiplication structure, with parameters learned through optimization.

4.2.1. Neural Network Architecture Design

We first present the architecture of the NN that will be utilized for tracking control. The NN structure is designed to (i) satisfy the input constraint $\mu(\cdot, k) \subseteq \mathcal{U}$, $k \in [0; N - 1]$, and (ii) to ensure that the control values generated by the NN match the the nominal control values when the states coincide with their nominal values $\{\tilde{x}_k\}_{k=0}^{N-1}$, that is, $\mu(\tilde{x}_k, k) = \tilde{u}_k$, $k \in [0; N - 1]$. To guarantee these properties, the architecture of μ is designed as follows. Consider a time step $k \in [0; N - 1]$. Let $\tilde{\mu}(\cdot, k) : \mathbb{R}^n \rightarrow \mathbb{R}^m$ be an l -layer feed-forward NN whose input is the state of the system (2) at time k , denoted by x_k . Then, we have $d_0 = n$ and $d_l = m$. Define $x_k^{(0)} = x_k - \tilde{x}_k$. We design the first $l - 2$ layers similar to the standard structure described in (1) as

$$\mathbf{L}_{k,j} : x_k^{(j)} = \phi(v_k^{(j)}) \quad \forall j \in [1; l - 2], \quad (5)$$

⁴In the computation of the BRSs, we consider a slightly inflated version of the disturbance set \mathcal{W} to provide a margin that increases the safe tracking capability of the learned NN controller.

with $v_k^{(j)} = W_{k,j} x_k^{(j-1)} + b_{k,j}$. The parameters $W_{k,j}$ and $b_{k,j}$ represent the weight and bias for layer $\mathbf{L}_{k,j}$, respectively, which are to be trained. For the $(l - 1)$ th layer, we set $d_{l-1} = d_0 = n$ and first introduce a multiplication operation linking the normalized input and $\mathbf{L}_{k,l-1}$ as

$$x_k^{(l-1)} = x_k^{(0)} \cdot * (W_{k,l-1} x_k^{(l-2)} + b_{k,l-1}). \quad (6)$$

Then, we define

$$\mathbf{L}_{k,l} : x_k^{(l)} = \Phi(W_{k,l} x_k^{(l-1)}) \quad (7)$$

with Φ being the *tanh* function and $W_{k,l} \in \mathbb{R}^{m \times n}$. Finally, the output is translated and scaled using a factor $R_{k,ul} \in \mathbb{R}^m$

$$\tilde{\mu}(x_k, k) = R_{k,ul} \cdot * x_k^{(l)} + \tilde{u}_k. \quad (8)$$

To retain the learning ability of the NN, the scaling factor $R_{k,ul}$ is set as a trainable parameter. With the above architecture, $\tilde{\mu}(\cdot, k)$ satisfies the following properties:

Lemma 2. *We have $\tilde{\mu}(\tilde{x}_k, k) = \tilde{u}_k$ and $\tilde{\mu}(x_k, k) \in [\tilde{u}_k - |R_{k,ul}|, \tilde{u}_k + |R_{k,ul}|]$.*

Proof 1. *If $x_k = \tilde{x}_k$, then $x_k^{(0)} = x_k - \tilde{x}_k = 0_n$. Correspondingly, $x_k^{(l-1)} = x_k^{(0)} \cdot * (W_{k,l-1} x_k^{(l-2)} + b_{k,l-1}) = 0_n$ and $x_k^{(l)} = \tanh(0_m) = 0_m$. By (8), we have $\tilde{\mu}(\tilde{x}_k, k) = \tilde{u}_k$. Also, since we use *tanh* as the activation function Φ in layer $\mathbf{L}_{k,l-1}$, limiting $x_k^{(l-1)}$ in the range $[-1_m, 1_m]$, we have $\tilde{\mu}(x_k, k) \in [\tilde{u}_k - |R_{k,ul}|, \tilde{u}_k + |R_{k,ul}|]$.*

Finally, to satisfy the input constraints, the control value $\mu(x_k, k)$ is obtained by trimming $\tilde{\mu}(x_k, k)$ as follows:

$$(\mu(x_k, k))_j = \begin{cases} (\tilde{\mu}(x_k, k))_j, & (\tilde{\mu}(x_k, k))_j \in [\underline{u}_j, \bar{u}_j], \\ \underline{u}_j, & (\tilde{\mu}(x_k, k))_j < \underline{u}_j, \\ \bar{u}_j, & (\tilde{\mu}(x_k, k))_j > \bar{u}_j, \end{cases}$$

$j \in [1; m]$. Note that since we employ the same network structure for all $k \in [0; N - 1]$, we omit the index k in the dimension d_i , $i \in [0; l]$ for brevity. We also note that the NN training is designed to optimize the performance of the intermediate controller, $\tilde{\mu}$, rather than that of the actual controller, μ . Empirical evidence indicates that, in the majority of cases, $\tilde{\mu}(x_k, k) \in \mathcal{U}$, ensuring that $\mu(x_k, k) = \tilde{\mu}(x_k, k)$. Consequently, additional clipping, as defined above, is rarely required and is only applied in exceptional scenarios where the inputs fall slightly outside the allowed range.

4.2.2. Sampling Methods for Training Data

Next, we discuss how we sample the states inside $\Lambda_k = \tilde{x}_k + G^k \mathbb{B}_{q_k}$ for time step $k \in [0; N - 1]$, to construct the training data set. Intuitively, the states near

the boundary of Λ_k are more deviated from the nominal trajectory, making them harder to drive towards \tilde{x}_{k+1} , $k \in [0; N - 1]$. To address this challenge during the learning process, we use both extreme sampling (points near boundary) and uniform sampling to construct the training sets \mathbf{S}_k as follows. For uniform sampling, we uniformly generate H_k^u points $\{r_i\}_{i=1}^{H_k^u}$ randomly from \mathbb{B}_{q_k} . The uniform sampling set is then defined as $\mathbf{S}_k^u \triangleq \{\tilde{x}_k + G^k r_i\}_{i=1}^{H_k^u}$. For extreme sampling, we generate H_k^{ex} data points to form set \mathbf{S}_k^{ex} . The sampling data set \mathbf{S}_k is then $\mathbf{S}_k = \mathbf{S}_k^u \cup \mathbf{S}_k^{ex}$. We randomly split \mathbf{S}_k into training set $\mathbf{S}_{k,train}$ and validation set $\mathbf{S}_{k,val}$. We denote the training points at time step k as $z_{k,h}$ for $h \in [1; H_k^{train}]$, and the validation points at time step k as $z_{k,h}$ for $h \in [1; H_k^{val}]$.

4.2.3. Optimization for Neural Network Training

For each $k \in [0; N - 1]$, the problem of training the NN tracking controller $\tilde{\mu}$ can be posed as the following optimization problem:

$$\text{minimize } P_k = \alpha_{k,1} P_{k,1} + \alpha_{k,2} P_{k,2}, \quad (9)$$

where we have two penalty terms $P_{k,1}$ and $P_{k,2}$ in the objective function, defined as

$$P_{k,1} = \frac{1}{H_k^{train}} \sum_{z_{k,h} \in \mathbf{S}_{k,train}} \left[\|d_{k,G}(z_{k,h})\|_\infty + \lambda \exp(\max(\|d_{k,G}(z_{k,h})\|_\infty - 1, 0)) \right], \quad (10)$$

with $d_{k,G}(\cdot) \triangleq (\tilde{G}^{k+1})^\dagger(f(\cdot, \tilde{\mu}(\cdot, k)) - \tilde{x}_{k+1})$, and

$$P_{k,2} = \|R_{k,ul}\|_1, \quad (11)$$

with $\lambda > 0$, $\alpha_{k,1} > 0$, $\alpha_{k,2} > 0$ being the respective weighting factors. Broadly speaking, the first term $P_{k,1}$ guides the state toward the consecutive backward reachable set, and the second term $P_{k,2}$ is concerned with the input being inside the allowed range. We examine the construction of each term below.

Penalty Term $P_{k,1}$: Note that for a given $k \in [0; N - 1]$ and state $x_k \in \Lambda_k$, if the control law $\tilde{\mu}$ ensures that $\|d_{k,G}(x_k)\|_\infty \leq 1$, then x_k is guaranteed to be driven to Λ_{k+1} under the closed-loop dynamics of (2), where the smaller the value of $\|d_{k,G}(x_k)\|_\infty$, the closer the next state is to \tilde{x}_{k+1} (the center of Λ_{k+1}). To see this, let $\tilde{b} = (\tilde{G}^{k+1})^\dagger(f(x_k, \tilde{\mu}(x_k, k)) - \tilde{x}_{k+1}) \in \mathbb{B}_{q_{k+1}}$; then $f(x_k, \tilde{\mu}(x_k, k)) = \tilde{x}_{k+1} + \tilde{G}^{k+1} \tilde{b} \in \tilde{\Lambda}_{k+1}$, and hence $f(x_k, \tilde{\mu}(x_k, k)) + \mathcal{W} \subseteq \Lambda_{k+1}$. Based on this fact, we penalize the norm itself and additionally include an exponential penalty if the norm exceeds 1. With training

points $z_{k,h}$, $h \in [1; H_k^{train}]$, which are sampled from Λ_k , we then have $P_{k,1}$ as in (10).

Penalty Term $P_{k,2}$: According to Lemma 2, $\tilde{\mu}(x_k, k) \in \llbracket \tilde{u}_k - |R_{k,ul}|, \tilde{u}_k + |R_{k,ul}| \rrbracket$. Effectively, $\|R_{k,ul}\|_1$ represents the deviation of control value generated by the NN from the nominal input \tilde{u}_k , which we penalize by including term $P_{k,2}$ as defined in (11).

Remark 2. *The learned neural network controller μ does not possess formal safe tracking guarantees. In principle, reachability analysis tools (such as those referenced in the Introduction) could be employed to verify its performance. However, the scalability of these methods is limited to low-dimensional systems and short time horizons, making them impractical for tracking applications, which typically involve a relatively large number of time steps. Therefore, in this work, we focus on formal safety verification of the NN-based tracking controller and provide statistical safety guarantees through conformal prediction.*

4.3. Formal Verification with Conformal Prediction

To obtain rigorous guarantees on tracking performance under disturbances, we utilize *formal verification* based on *conformal prediction*, which is a nonparametric framework to provide distribution-free confidence sets for general machine learning models [39–41]. Conformal prediction offers a unified framework for designing safe controllers and performing offline verification of learning-enabled autonomous systems, while maintaining scalability, interpretability, and formal guarantees [42]. This approach is especially well-suited for safety-critical systems, as it offers finite-sample coverage guarantees under mild assumptions.

We apply the standard full conformal prediction procedure to verify whether closed-loop trajectories satisfy the reach-avoid specification with a desired confidence level. Specifically, we first construct forward safe sets $\mathcal{S}_k \subseteq \mathcal{X}_o \setminus \mathcal{X}_u$, $k \in [0; N - 1]$, as follows. For each time step $k \in [0; N - 1]$, we define $\mathcal{S}_k \subset \mathbb{R}^n$ as an axis-aligned hyper-rectangle, containing the nominal state \tilde{x}_k and ensuring that all states within \mathcal{S}_k remain in the operating region \mathcal{X}_o and avoid the unsafe set \mathcal{X}_u . We parameterize \mathcal{S}_k by one-sided half-widths vectors $r_k^+, r_k^- \in \mathbb{R}_+^n$ representing the maximal allowable displacements from the nominal state \tilde{x}_k for each coordinate in the positive and negative directions respectively. Each axis $j \in \{1, \dots, n\}$ is categorized to either be a separating coordinate or a non-separating coordinate. The corresponding $(r_k^+)_j, (r_k^-)_j \in \mathbb{R}_+$ are then determined by the distance between the nominal coordinate $(\tilde{x}_k)_j$ and

the nearest boundaries of \mathcal{X}_o and \mathcal{X}_u . Specifically,

$$\mathcal{S}_k \triangleq \llbracket \tilde{x}_k - r_k^-, \tilde{x}_k + r_k^+ \rrbracket, \quad (12)$$

For separating coordinate j , we set

$$\begin{aligned} (r_k^+)_j &= \min \left\{ (\bar{x}_o)_j - (\tilde{x}_k)_j, \min_{i \in \mathcal{A}_{k,j}^+} \left\{ (\underline{x}_u^{(i)})_j - (\tilde{x}_k)_j \right\} \right\} - \varepsilon, \\ (r_k^-)_j &= \min \left\{ (\tilde{x}_k)_j - (\underline{x}_o)_j, \min_{i \in \mathcal{A}_{k,j}^-} \left\{ (\tilde{x}_k)_j - (\bar{x}_u^{(i)})_j \right\} \right\} - \varepsilon, \end{aligned} \quad (13)$$

where the active index sets are defined as $\mathcal{A}_{k,j}^+ \triangleq \{i : (\underline{x}_u^{(i)})_j - (\tilde{x}_k)_j > 0\}$ and $\mathcal{A}_{k,j}^- \triangleq \{i : (\tilde{x}_k)_j - (\bar{x}_u^{(i)})_j > 0\}$.

For non-separating coordinate j , we set

$$\begin{aligned} (r_k^+)_j &= (\bar{x}_o)_j - (\tilde{x}_k)_j - \varepsilon \\ (r_k^-)_j &= (\tilde{x}_k)_j - (\underline{x}_o)_j - \varepsilon, \end{aligned} \quad (14)$$

Here, $\varepsilon > 0$ is a small safety margin to maintain strict separation from obstacle boundaries. In practice, we select separating coordinates and non-separating coordinates such that $(r_k^+)_j \geq 0, (r_k^-)_j \geq 0, \forall k \in [0; N-1], \forall j \in [1; n]$. Then, \mathcal{S}_k is guaranteed to be strictly separated from $\mathcal{X}_o \setminus \mathcal{X}_u$.

Lemma 3. *For any given $k \in [0; N-1]$, suppose there exists at least one coordinate $j^s \in \{1, \dots, n\}$ such that the corresponding \mathcal{S}_k and every obstacle $\mathcal{X}_u^{(i)}$ are strictly disjoint, i.e., for $\forall i \in [1; N_u]$,*

$$\left[(\tilde{x}_k)_{j^s} - (r_k^-)_{j^s}, (\tilde{x}_k)_{j^s} + (r_k^+)_{j^s} \right] \cap \left[(\underline{x}_u^{(i)})_{j^s}, (\bar{x}_u^{(i)})_{j^s} \right] = \emptyset. \quad (15)$$

If, in addition, the one-sided half-widths satisfy $(r_k^+)_j \geq 0$ and $(r_k^-)_j \geq 0$ for all $j \in [1; n]$, then it is guaranteed

$$\mathcal{S}_k \subseteq \mathcal{X}_o, \mathcal{S}_k \cap \mathcal{X}_u^{(i)} = \emptyset, \quad \forall i \in [1; N_u]. \quad (16)$$

Remark 3. *By Assumption 2, the nominal trajectories satisfy $\tilde{x}_k \in \mathcal{X}_o \setminus \mathcal{X}_u, \forall i \in [1; N_u], k \in [0; N]$. Therefore, the conditions in Lemma 3 are naturally satisfied.*

The resulting sets act as trajectory-level safety certificates in the sense that any trajectory $\tau = (x_0, x_1, \dots, x_N)$ is guaranteed to satisfy the reach-avoid specification if

$$x_k \in \mathcal{S}_k \text{ for all } k \in [0; N-1], \quad \text{and} \quad x_N \in \mathcal{X}_t.$$

Then, to numerically encode specification violations, we define the stepwise violation at time step k as

$$s_k \triangleq \begin{cases} \text{dist}(x_k, \mathcal{S}_k) & \text{if } k \in [0; N-1], \\ \text{dist}(x_N, \mathcal{X}_t) & \text{if } k = N, \end{cases} \quad (17)$$

where $\text{dist}(x, \mathcal{A}) \triangleq \inf_{y \in \mathcal{A}} \|x - y\|_2$. We then have the *trajectory-level nonconformity score* defined as the accumulated violation

$$s(\tau) \triangleq \sum_{k=0}^N s_k. \quad (18)$$

Consequently, $s(\tau) = 0$ if and only if the trajectory τ passes the safety certificate over the horizon. Larger values of $s(\tau)$ indicate greater overall violation.

Now, let $\{\tau_h\}_{h=1}^{H_0^{\text{test}}}$ be a test set of closed-loop trajectories, each generated by applying the tracking controller to the system (2) with random initial condition $x_{0,h} \in \Lambda_0$ and disturbance sequence $\{w_{k,h}\}_{k=1}^N \subseteq \mathcal{W}^N$. Each trajectory $\tau_h = (x_{0,h}, x_{1,h}, \dots, x_{N,h})$ yields a score $s(\tau_h)$.

Assumption 3. *The initial conditions $x_0^{(i)} \sim \Lambda_0$ are drawn independently, and the disturbances $w_k^{(i)} \sim \mathcal{W}$ are independent across time and rollouts.*

Under this scheme, the resulting trajectories τ_i are independent thus exchangeable random elements [43] in the trajectory space, satisfying the conditions to apply conformal prediction to this problem.

Then, we compute a quantile threshold to certify any unseen (future) trajectory. Let the scores $\{s(\tau_h)\}_{h=1}^{H_0^{\text{test}}}$ be sorted in ascending order as $s_{(1)} \leq \dots \leq s_{(H_0^{\text{test}})}$. For a confidence level $1 - \delta$, where δ is user-defined, we define the empirical quantile $q_{1-\delta} \triangleq s_{(l)}$ with $l = \lceil (1-\delta)(H_0^{\text{test}} + 1) \rceil$. Denote τ_{new} to be a future rollout with initial state and disturbance $(x_{0,\text{new}}, \{w_{k,\text{new}}\}_{k=0}^{N-1})$ and associated score to be $s(\tau_{\text{new}})$. We have the result below.

Proposition 1 (Reach-Avoid Guarantee [42]). *Under Assumption 3, the trajectory τ_{new} satisfies*

$$\mathbb{P}[s(\tau_{\text{new}}) \leq q_{1-\delta}] \geq 1 - \delta. \quad (19)$$

This provides a certified formal statistical safety guarantee for the tracking controller, purely from sampled trajectories, without requiring knowledge of the distribution over initial conditions or disturbances.

5. Experiments

Consider the discrete-time Dubin's car system:

$$\begin{pmatrix} (x_{k+1})_1 \\ (x_{k+1})_2 \\ (x_{k+1})_3 \end{pmatrix} \in \begin{pmatrix} (x_k)_1 + \tau_s (u_k)_1 \cos((x_k)_3) \\ (x_k)_2 + \tau_s (u_k)_1 \sin((x_k)_3) \\ (x_k)_3 + \tau_s (u_k)_2 \end{pmatrix} + \mathcal{W},$$

where $((x_k)_1, (x_k)_2)$ denotes the car position, $(x_k)_3$ denotes the heading angle, τ_s is the sampling time ($\tau_s = 0.05$), $(u_k)_1$ and $(u_k)_2$ are control inputs corresponding

to the car speed and turning rate, respectively, and the disturbance set is given by $\mathcal{W} = \tau_s([-0.02, 0.02]^2 \times [-0.1, 0.1])$. We now demonstrate how our approach can be used to synthesize a NN tracking controller that keeps the system states in the operating domain $\mathcal{X}_o = [0, 5] \times [0, 2] \times [-\pi/2, \pi/2]$, while avoiding the unsafe set $(([1.5, 3] \times [0, 0.5]) \cup ([1.5, 2.5] \times [1, 2]) \cup ([3.5, 4.5] \times [0, 1])) \times [-\pi/2, \pi/2]$, and steering the system's states to the target set $\mathcal{X}_t = [3.5, 5] \times [1.5, 2] \times [-\pi/5, \pi/5]$, using control values in the set $\mathcal{U} = [-8, 8] \times [-5, 5]$. The initial set \mathcal{X}_i is singleton, corresponding to a starting point, that is assigned different values discussed shortly.

For each starting point value, we calculate a nominal trajectory, using a sampling-based approach (RRT), and obtain under-approximate BRSs along the nominal trajectory. We carry out the zonotopic computations, the zonotopic plots, and the sampling from zonotopes using the reachability toolbox CORA [44].

The NN controller μ is trained as follows. At time step k , we generate $H_k^u = 40$ points for the uniform sampling set \mathbf{S}_k^u and $H_k^{ex} = 60$ points for the extreme sampling set \mathbf{S}_k^{ex} using command `randPoint`[44]. The entire sampling set $\mathbf{S}_k = \mathbf{S}_k^u \cup \mathbf{S}_k^{ex}$ is then randomly split into training set $\mathbf{S}_{k,train}$ and validation set $\mathbf{S}_{k,val}$ at a ratio of 7:3, with $H_k^{train} = 70$ and $H_k^{val} = 30$. During the training, validation is conducted every 200 epochs, and the training is terminated if there is no further improvement on the loss for 5 consecutive validations, with the validation loss being $\frac{1}{H_k^{val}} \sum_{z_{k,h} \in \mathbf{S}_{k,val}} \|d_{k,G}(z_{k,h})\|_\infty$ for time step k . In the objective function, we set $\lambda = 0.1$, $\alpha_{k,1} = 10$, and $\alpha_{k,2} = 0.01$.

For the Dubin's car, $n = 3$ and $m = 2$. Correspondingly, we set the number of neurons for each layer to be $d_0 = d_5 = 3$, $d_1 = d_2 = d_3 = d_4 = 32$, and $d_6 = 2$. The activation function ϕ in the first $l - 2$ layers is ReLU. We apply Kaiming initialization [45] for the weights and zero initialization for the biases. The training is performed using the Adam optimizer with a learning rate of 3×10^{-4} and a weight decay of 10^{-4} on a local machine equipped with a 13th Gen Intel® Core™ i7-1360P processor featuring 12 parallel computing cores⁵. For formal verification, we set the safety margin in (13), (14) to be $\varepsilon = 0.01$ and perform the analysis under the same experimental setting.

To demonstrate the consistent performance of our NN controllers, we conduct experiments on three cases with different starting points $[4, 0.5, -\pi/4]^\top$, $[0.5, 4.5, \pi/4]^\top$,

and $[1, 1, 0]^\top$ respectively. For the three cases, we report the training time to be 8 minutes 35 seconds, 8 minutes 33 seconds, and 7 minutes 11 seconds respectively.

5.1. Consistent and Reliable Performance of Online Neural Network Tracking Controllers

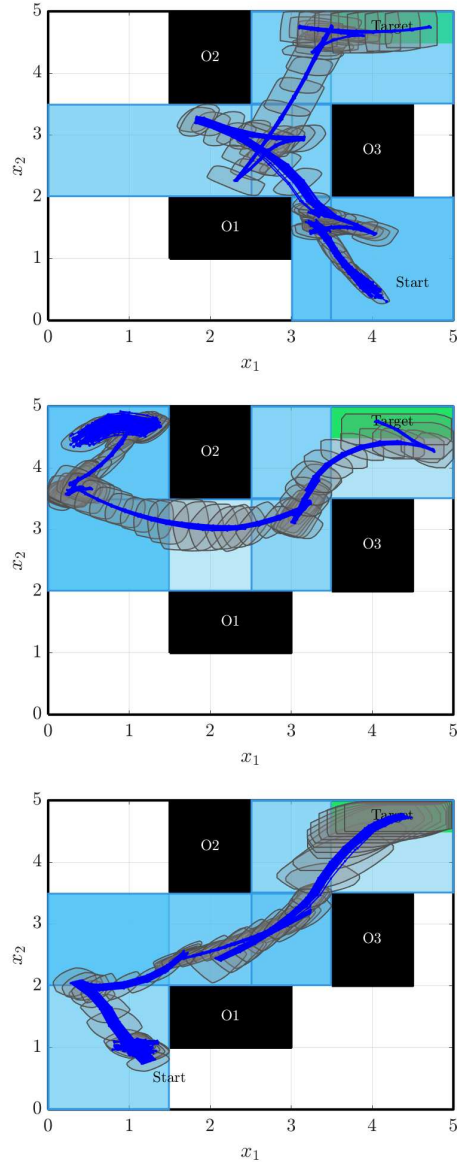


Figure 1: O_1, O_2, O_3 are obstacles to avoid and the green set is the target set. The nominal starting points \bar{x}_0 are: $[4, 0.5, -\pi/4]^\top$, $[0.5, 4.5, \pi/4]^\top$, and $[1, 1, 0]^\top$ respectively. For visual clarity, only 100 trajectories are shown out of 1000 simulated.

With the trained NN controllers, we have a closed-form mapping from the states to the inputs. In other words, regardless of the starting points within Λ_0 , we

⁵The code for all experiments is located in the Github repository: <https://github.com/YuezhuXu/Learning-NN-Safe-Tracking-Controllers-from-Backward-Reachable-Sets>

eliminate the need to solve any optimization problem during execution, thus significantly enhancing computational efficiency for online control applications. To evaluate the performance of the trained controllers, we apply the full conformal prediction method described in Section 4.3 for all three cases. As outlined in (12)-(14), we set the first and second dimension to be the separating coordinates and the third dimension to be the non-separating coordinate. We then construct forward safe sets $\{\mathcal{S}_k\}_{k=0}^N$ as axis-aligned hyper-rectangles centered at the nominal states $\{\tilde{x}_k\}_{k=0}^{N-1}$, guaranteed to lie within the operating domain \mathcal{X}_0 and avoid the unsafe set \mathcal{X}_u (the series of light blue boxes in Fig. 1). These sets act as safety certificates for each step. For each case, we simulate $H_0^{test} = 1000$ closed-loop trajectories $\{\tau_h\}_{h=1}^{H_0^{test}}$ under the fixed NN controller. The initial states $\{x_{0,h}\}_{h=1}^{H_0^{test}}$ are uniformly sampled from the corresponding initial zonotope $\Lambda_0 = \tilde{x}_0 + G^0\mathbb{B}_{q_0}$, using the `randPoint` command with the sampling type set to 'uniform'. The disturbance is drawn independently at each step following the uniform distribution $\mathcal{W} = \mathbf{U}(-a, a)$, where $a = [0.003, 0.003, 0.015]^T$. For each case, we check that all 1000 simulated trajectories stay inside \mathcal{S}_k at stage k , $\forall k \in [0; N-1]$ and reach \mathcal{X}_t at last, i.e., $s_k = 0$, $\forall k \in [0; N]$. According to (17)-(18), for our experiments, we obtain,

$$s(\tau_h) = 0, \quad \forall h \in [1; 1000]. \quad (20)$$

As a result, the sorted scores are $s_{(1)} = \dots = s_{(1000)} = 0$. To construct a conformal certification rule with confidence level 99.9%, $\delta = 0.001$, we compute

$$l = \lceil (1 - \delta)(H_0^{test} + 1) \rceil = \lceil 0.999 \cdot 1001 \rceil = 1000, \quad (21)$$

meaning that $q_{0.999} = s_{(1000)} = 0$. Therefore, according to Proposition 1, a future rollout τ_{new} has $s(\tau_{new}) \leq q_{0.999} = 0$. In other words, any τ_{new} is certified to stay inside the forward safe sets \mathcal{S}_k at stage k , $\forall k \in [0; N-1]$ and reach \mathcal{X}_t at last, thus satisfying the reach-avoid specification, at 99.9% confidence. In fact, owing to the learning ability of the NN controller, we manage to guide the states towards the center of zonotope for the next time step, resulting in different trajectories contracting to the nominal trajectory as the system evolves. Meanwhile, the simulation time for each trajectory is approximately 0.0270 seconds, 0.0245 seconds, and 0.0220 seconds respectively for the three cases. Note that if controls need to be generated for multiple initial states, there is potential for even faster implementation by leveraging parallel computing.

5.2. Extending beyond Backward Reachable Sets

Here, we demonstrate that the NN controller can have larger starting sets than optimization-based tracking controllers with BRSs. In other words, our NN controller is able to safely drive points outside Λ_0 to the target set. This highlights the strong generalization ability of the NN controllers in achieving superior tracking. To illustrate this, we enlarge the scale of the initial zonotope $\Lambda_0 = \tilde{x}_0 + G^0\mathbb{B}_{q_0}$ for the case of the starting point $[0.5, 4.5, -\pi/4]^T$ by 10%, 20%, 30%, and 50% respectively. The enlarged zonotopes are written as $\Lambda_0^\zeta = \tilde{x}_0 + (1 + \zeta)G^0\mathbb{B}_{q_0}$, with ζ selected as 0.1, 0.2, and 0.3. Then we sample from Λ_0^ζ uniformly to obtain 1000 test points for each ζ . In Fig. 2, we mark the trajectories for $\zeta = 0.1, 0.2, 0.3$ with color red, and brown separately. We include an inset in each plot to highlight the initial zonotope and the distribution of starting points sampled. Clearly, from Fig. 2, many initial points sampled are outside Λ_0 for $\zeta = 0.1, 0.2$, and 0.3. We observe that all 1000 rollouts in each enlarged case ζ remain inside the safe sets \mathcal{S}_k (the series of light blue boxes same as the ones in Section 5.1) for $\forall k \in [0; N-1]$ and reach the target set \mathcal{X}_t , meaning that each trajectory still achieves $s_k^S = 0$ for all k , and thus

$$s^S(\tau_h) = 0, \quad \forall h \in [1; 1000].$$

This again implies that the sorted scores satisfy $s_{(1)}^S = \dots = s_{(1000)}^S = 0$. For each ζ , we set $\delta = 0.001$ to construct a conformal predictor at 99.9% confidence, and compute the quantile

$$l = \lceil (1 - \delta)(n + 1) \rceil = \lceil 0.999 \cdot 1001 \rceil = 1000,$$

with $q_{0.999} = s_{(1000)} = 0$. Therefore, for each enlarged initial set Λ_0^ζ , any future rollout τ_{new}^S is certified to satisfy $s^S(\tau_{new}^S) \leq 0$, thus meeting the reach-avoid specification, with 99.9% confidence. The simulation time for each trajectory remains low, being approximately 0.0252 seconds, 0.0258 seconds, and 0.0263 seconds, respectively for $\tau = 0.1, 0.2$, and 0.3.

Next, we benchmark the performance of the NN controllers against the optimization-based controller from [7]. We consider the case of the starting nominal point $[1, 1, 0]^T$ and pick an initial point $[1, 0.8, 0]^T$ outside Λ_0 . The optimization-based controller from [7] fails in the sense that it cannot find a control value that drives the initial value to Λ_1 . Starting from the same position, we apply trained NN tracking controller which manages to safely drive the state to the target set, even when the starting point is outside Λ_0 as shown in Fig. 3.

This provides empirical evidence suggesting that with the use of NN controllers, safe sets can be expanded well beyond the theoretical guarantees provided

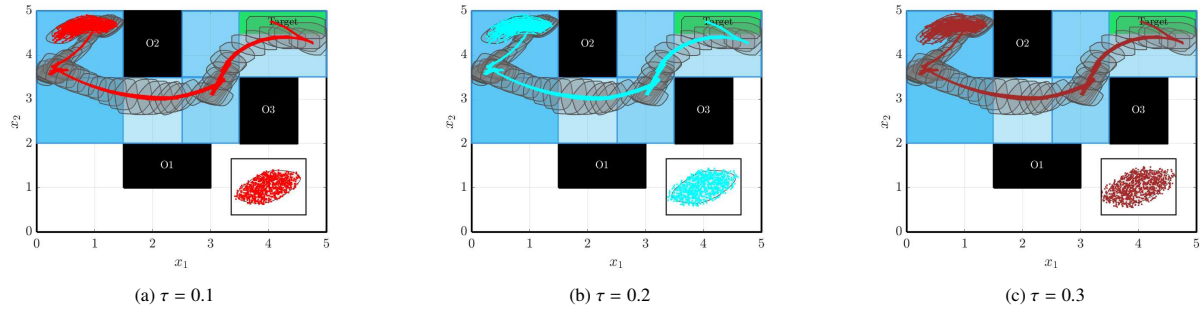


Figure 2: Trajectories generated with the initial states uniformly sampled from the enlarged initial zotopes Λ_0^r . For visual clarity, only 100 trajectories are shown out of 1000 simulated for each case. The original initial zotopes and the sampled initial states are highlighted in the inset in each plot.

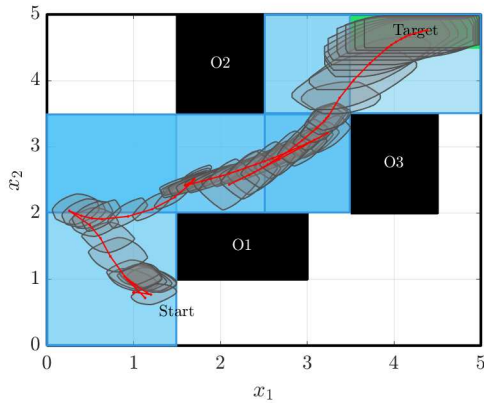


Figure 3: O_1, O_2, O_3 are obstacles to avoid and the green set is the target set. The nominal starting points is $[1, 1, 0]^T$ and the initial point we pick outside Λ_0 is $[1, 0.8, 0]^T$.

by classical backward reachability based control designs, motivating the need for further research in closing the gap between provable guarantees and the tracking performance observed in practice.

6. Discussion and Future Work

In this work, we presented a NN-based safe tracking control framework for nonlinear discrete-time systems with reach-avoid specifications in the presence of disturbances. Our approach relies on nominal trajectory generation and computations of safe zotopic BRSs along the nominal trajectory. The computed BRSs are then used to guide the training of a NN tracking controller, such that the NN drives the system's states through these BRSs, thus increasing the likelihood of safe reachability. We also provide statistical guarantees on the safe tracking capabilities of the learned NN controller with a high confidence level of 99.9%. Motivated by this work, we aim to explore several research directions in the future. One of the direction is refining the computation

of BRSs such as those in [7] so that they can better aid NN tracking control by providing larger sets of training points. We will also explore new BRS-informed NN architecture designs that can potentially provide better tracking capabilities.

References

- [1] K. Graichen, M. Treuer, M. Zeitz, Swing-up of the double pendulum on a cart by feedforward and feedback control with experimental validation, *Automatica* 43 (1) (2007) 63–71.
- [2] T. Lee, M. Leok, N. H. McClamroch, Geometric tracking control of a quadrotor uav on se (3), in: *Proc. of CDC, IEEE*, 2010, pp. 5420–5425.
- [3] S. Fukuda, Y. Satoh, O. Sakata, Trajectory-tracking control considering obstacle avoidance by using control barrier function, in: *Proc. of CACS, IEEE*, 2020, pp. 1–6.
- [4] W. Langson, I. Chrysochoos, S. Raković, D. Q. Mayne, Robust model predictive control using tubes, *Automatica* 40 (1) (2004) 125–133.
- [5] S. Singh, B. Landry, A. Majumdar, J.-J. Slotine, M. Pavone, Robust feedback motion planning via contraction theory, *The International Journal of Robotics Research* (2019).
- [6] P. Zhao, A. Lakshmanan, K. Ackerman, A. Gahlawat, M. Pavone, N. Hovakimyan, Tube-certified trajectory tracking for nonlinear systems with robust control contraction metrics, *IEEE Robotics and Automation Letters* 7 (2) (2022) 5528–5535.

- [7] M. Serry, L. Yang, N. Ozay, J. Liu, Safe tracking control of discrete-time nonlinear systems using backward reachable sets, in: 2024 American Control Conference (ACC)(Accepted), 2024.
- [8] L. Yang, N. Ozay, Scalable zonotopic under-approximation of backward reachable sets for uncertain linear systems, *IEEE Control Systems Letters* 6 (2021) 1555–1560.
- [9] L. Yang, H. Zhang, J.-B. Jeannin, N. Ozay, Efficient backward reachability using the minkowski difference of constrained zonotopes, *IEEE Trans. Computer-Aided Design of Integrated Circuits and Systems* 41 (11) (2022) 3969–3980.
- [10] S. Arora, N. Cohen, E. Hazan, On the optimization of deep networks: Implicit acceleration by over-parameterization, in: International conference on machine learning, PMLR, 2018, pp. 244–253.
- [11] A. Abate, D. Ahmed, M. Giacobbe, A. Peruffo, Formal synthesis of lyapunov neural networks, *IEEE Control Systems Letters* 5 (3) (2020) 773–778.
- [12] J. Liu, Y. Meng, M. Fitzsimmons, R. Zhou, Tool lyznet: A lightweight python tool for learning and verifying neural lyapunov functions and regions of attraction, in: Proceedings of the 27th ACM International Conference on Hybrid Systems: Computation and Control, 2024, pp. 1–8.
- [13] Y. Xu, S. Sivaranjani, Learning dissipative neural dynamical systems, *IEEE Control Systems Letters* 7 (2023) 3531–3536.
- [14] S. Chen, M. Fazlyab, M. Morari, G. J. Pappas, V. M. Preciado, Learning region of attraction for nonlinear systems, in: 2021 60th IEEE Conference on Decision and Control (CDC), IEEE, 2021, pp. 6477–6484.
- [15] Y.-C. Chang, N. Roohi, S. Gao, Neural lyapunov control, *Advances in neural information processing systems* 32 (2019).
- [16] J. Wu, A. Clark, Y. Kantaros, Y. Vorobeychik, Neural lyapunov control for discrete-time systems, *Advances in neural information processing systems* 36 (2023) 2939–2955.
- [17] N. Hassan, A. Saleem, Neural network-based adaptive controller for trajectory tracking of wheeled mobile robots, *IEEE Access* 10 (2022) 13582–13597.
- [18] D. Wang, D. Liu, C. Mu, Y. Zhang, Neural network learning and robust stabilization of nonlinear systems with dynamic uncertainties, *IEEE transactions on neural networks and learning systems* 29 (4) (2017) 1342–1351.
- [19] H. Dai, B. Landry, L. Yang, M. Pavone, R. Tedrake, Lyapunov-stable neural-network control, arXiv preprint arXiv:2109.14152 (2021).
- [20] S. Talukder, R. Kumar, Robust stability of neural-network-controlled nonlinear systems with parametric variability, *IEEE Transactions on Systems, Man, and Cybernetics: Systems* 53 (8) (2023) 4820–4832.
- [21] Y. Zhang, H. Zhang, X. Xu, Reachability analysis of neural network control systems with tunable accuracy and efficiency, *IEEE Control Systems Letters* (2024).
- [22] M. Everett, G. Habibi, C. Sun, J. P. How, Reachability analysis of neural feedback loops, *IEEE Access* 9 (2021) 163938–163953.
- [23] M. Everett, G. Habibi, J. P. How, Efficient reachability analysis of closed-loop systems with neural network controllers, in: 2021 IEEE International Conference on Robotics and Automation (ICRA), IEEE, 2021, pp. 4384–4390.
- [24] Y. Zhang, H. Zhang, X. Xu, Backward reachability analysis of neural feedback systems using hybrid zonotopes, *IEEE Control Systems Letters* 7 (2023) 2779–2784.
- [25] W. Xiang, D. M. Lopez, P. Musau, T. T. Johnson, Reachable set estimation and verification for neural network models of nonlinear dynamic systems, *Safe, autonomous and intelligent vehicles* (2019) 123–144.
- [26] S. Chen, V. M. Preciado, M. Fazlyab, One-shot reachability analysis of neural network dynamical systems, in: 2023 IEEE International Conference on Robotics and Automation (ICRA), IEEE, 2023, pp. 10546–10552.
- [27] S. Sharifi, M. Fazlyab, Provable bounds on the hessian of neural networks: Derivative-preserving reachability analysis, arXiv preprint arXiv:2406.04476 (2024).

- [28] H. Zhang, Y. Zhang, X. Xu, Hybrid zonotope-based backward reachability analysis for neural feedback systems with nonlinear plant models, in: 2024 American Control Conference (ACC), IEEE, 2024, pp. 4155–4161.
- [29] J. A. Siefert, T. J. Bird, A. F. Thompson, J. J. Glunt, J. P. Koeln, N. Jain, H. C. Pangborn, Reachability analysis using hybrid zonotopes and functional decomposition, *IEEE Transactions on Automatic Control* (2025).
- [30] L. Koller, T. Ladner, M. Althoff, Set-based training for neural network verification, *arXiv preprint arXiv:2401.14961* (2024).
- [31] L. K. Chung, A. Dai, D. Knowles, S. Kousik, G. X. Gao, Constrained feedforward neural network training via reachability analysis, *arXiv preprint arXiv:2107.07696* (2021).
- [32] A. Harapanahalli, S. Coogan, Certified robust invariant polytope training in neural controlled odes, *arXiv preprint arXiv:2408.01273* (2024).
- [33] A. Girard, Reachability of uncertain linear systems using zonotopes, in: *Proc. of HSCC*, Vol. 3414, Springer, 2005, pp. 291–305.
- [34] S. M. LaValle, J. J. Kuffner Jr, Randomized kinodynamic planning, *The international journal of robotics research* 20 (5) (2001) 378–400.
- [35] V. Kurtz, H. Lin, Trajectory optimization for high-dimensional nonlinear systems under STL specifications, *IEEE Control Systems Letters* 5 (4) (2020) 1429–1434.
- [36] J. Chen, W. Zhan, M. Tomizuka, Autonomous driving motion planning with constrained iterative lqr, *IEEE Transactions on Intelligent Vehicles* 4 (2) (2019) 244–254.
- [37] Y. Zhao, H.-C. Lin, M. Tomizuka, Efficient trajectory optimization for robot motion planning, in: 2018 15th international conference on control, automation, robotics and vision (ICARCV), IEEE, 2018, pp. 260–265.
- [38] A. Sasfi, M. N. Zeilinger, J. Köhler, Robust adaptive mpc using control contraction metrics, *Automatica* 155 (2023) 111169.
- [39] V. Vovk, A. Gammerman, G. Shafer, *Algorithmic learning in a random world*, Springer, 2005.
- [40] G. Shafer, V. Vovk, A tutorial on conformal prediction., *Journal of Machine Learning Research* 9 (3) (2008).
- [41] A. N. Angelopoulos, S. Bates, et al., Conformal prediction: A gentle introduction, *Foundations and trends® in machine learning* 16 (4) (2023) 494–591.
- [42] L. Lindemann, Y. Zhao, X. Yu, G. J. Pappas, J. V. Deshmukh, Formal verification and control with conformal prediction, *arXiv preprint arXiv:2409.00536* (2024).
- [43] J. M. Bernardo, The concept of exchangeability and its applications, *Far East Journal of Mathematical Sciences* 4 (1996) 111–122.
- [44] M. Althoff, An introduction to CORA 2015, in: *Proc. of ARCH*, 2015.
- [45] K. He, X. Zhang, S. Ren, J. Sun, Delving deep into rectifiers: Surpassing human-level performance on imagenet classification, in: *Proceedings of the IEEE international conference on computer vision*, 2015, pp. 1026–1034.